Journal of Power Sources 241 (2013) 87–93

Contents lists available at SciVerse ScienceDirect

Journal of Power Sources

journal homepage: www.elsevier.com/locate/jpowsour

Prolongation of lifetime of high temperature proton exchange membrane fuel cells

Yuka Oono [a,*], Atsuo Sounai [b], Michio Hori [a]

[a] Fuel Cell Research Center, Daido University, 10-3 Takiharu-cho, Minami-ku, Nagoya, Aichi 457-8530, Japan
[b] Dept. of Materials Science & Engineering, Suzuka National College of Technology, Shirako-cho, Suzuka, Mie 510-0294, Japan

HIGHLIGHTS

- In-situ endurance tests were conducted on HT-PEMFC with ABPBI membrane.
- Cell voltage decrease of the cell with ABPBI membrane was only 4.4% for 17,500 h.
- Post analyses were performed on both the 1000 and 17,500 h cells.
- Catalyst layers maintained the original amount of phosphoric acid during 17,500 h.
- The membrane maintained its original thickness and acid during 17,500 h.

ARTICLE INFO

Article history:
Received 12 December 2012
Received in revised form
1 March 2013
Accepted 25 March 2013
Available online 12 April 2013

Keywords:
High-temperature proton exchange membrane fuel cells
Performance
Durability
ABPBI
Phosphoric acid
Mechanism

ABSTRACT

In a previous study on the long-term operation of high-temperature proton exchange membrane fuel cells (HT-PEMFCs) with polybenzimidazole (PBI) membranes, it was found that the main cause of the observed decrease in cell voltage with time was phosphoric acid depletion due to evaporation. Based on this result, in the present study, the effects of using a different kind of cell membrane were investigated. Instead of PBI membranes, phosphoric-acid-doped, chemically cross-linked poly(2,5-benzimidazole) (ABPBI) membranes were employed in HT-PEMFCs and long-term power generation tests were carried out. Two separate cells were operated for 1000 and 17,500 h at a temperature of 150 °C and a current density of 0.2 A cm^{-2}. Their membrane electrode assemblies were then subjected to electron probe microanalysis. The results for the cell operated for 17,500 h were directly compared with those for a cell with a PBI membrane operated for 17,800 h in a previous study, allowing the mechanism of cell performance reduction in HT-PEMFCs to be further elucidated.

1. Introduction

Fuel cells have attracted attention as an environmentally friendly, clean energy source and have been the subject of a large amount of research. At present, the most actively studied fuel cells are perfluorosulfonic acid-type low-temperature proton exchange membrane fuel cell (LT-PEMFCs). LT-PEMFC are different to previous generation fuel cells in that they use a solid polymer membrane as the electrolyte, with water as the proton conduction medium, and can therefore operate at temperatures below 100 °C. Consequently, they have widened the range of applications of fuel cells to include small-scale power sources for automobiles, homes and portable devices, and such applications are expected to expand in the future. A recent trend in Japan is the commercialization of 1-kW class domestic cogeneration systems that use both electricity and electrically generated waste heat, made possible by significant improvements in fuel cell performance and durability [1]. However, a major stumbling block for commercialization is that such systems tend to be very complex and expensive, because LT-PEMFCs inherently require humidification to allow proton conduction via water. In addition, system efficiency is relatively low due to the low operating temperature of <100 °C [1], and a CO selective oxidizer is required since the CO tolerance of the electrode catalyst is reduced at low temperature [2–4].

Research on the next generation of PEMFCs is currently underway, and it is hoped that these problems can be resolved by simplification of the system, reduction of the production cost, and

* Corresponding author. Tel.: +81 52 612 6111x5621; fax: +81 52 612 5623.
E-mail address: oono-y@daido-it.ac.jp (Y. Oono).

0378-7753/$ – see front matter © 2013 Elsevier B.V. All rights reserved.
http://dx.doi.org/10.1016/j.jpowsour.2013.03.122

improvement of the efficiency at operating temperatures of 135–160 °C [5]. An additional requirement is that the PEMFCs have sufficient high temperature tolerance in the absence of humidification, and be based on polymer electrolytic membranes that can be chemically coupled with acids capable of proton conduction. To this end, research has been carried out on acids that are capable of proton conduction at temperatures above 100 °C, in addition to acid-absorbing polymers [6–8]. The results suggest that both sulfuric and phosphoric acids have a high proton conduction capability [9]. With regard to the polymers used for the membranes, fundamental studies have been carried out on polybenzimidazole (PBI) [10], polyethylene oxide [11], polyvinyl alcohol [12,13], polyacrylamide [14] and polyethylene imine [15].

Investigations have been carried out on HT-PEMFCs based on phosphoric-acid-doped chemically cross-linked poly (2.5-benzimidazole) (ABPBI) and PBI membranes, from and the viewpoint of not only the membrane conductivity and heat resistance [16,17], but also the power generation capability of actual cells [18–22]. Zhang et al. reported that higher cell performance was achieved as the operating temperature approached 200 °C [22]. In addition, lifetimes exceeding 10,000 h have been reported by research groups at BASF and Samsung [23,24], and these PEMFCs are considered to be closest to commercial viability.

However, there have been very few reports on the mechanism underlying the deterioration of such cells using PBI and ABPBI membranes [16]. Although one study has been carried out on the reduction in performance during 500 h of operation at 150 °C [21], very little has been reported concerning the causes of cell deterioration over longer periods. Based on long-term power generation tests exceeding two years, the present authors clarified the deterioration mechanism in HT-PEMFCs and showed that lifetimes exceeding 20,000 h can be achieved by improving the stability of the electrolyte membrane [25].

In the present study, as part of a series of investigations on the durability of HT-PEMFCs [25,26], long-term power generation tests were carried out on cells using ABPBI membranes rather than the PBI membranes used in a previous study [25]. The ABPBI membranes were pre-doped with phosphoric acid [16,27,28] and were expected to be more stable than PBI membranes due to the presence of cross-linking. The purpose of this study was thus to investigate whether the stability of the membrane itself is the main factor influencing cell deterioration for operation times up to 20,000 h. Two such ABPBI membranes were used in HT-PEMFCs and operated for 1000 and 17,500 h. The membrane electrode assembly (MEA) was then removed from the cells and evaluated using electron probe microanalysis (EPMA). To clarify the effect of the membrane on cell deterioration, the electrical and EPMA results for the ABPBI containing cell tested for 17,500 h in the present study were compared with those for the PBI-based cell tested for 17,800 h in a previous study [25].

2. Experimental

2.1. Acid-doping

Eight ABPBI membranes with an area of 2 × 2 cm^2 and a thickness of approximately 40 μm were prepared, and their weights and dimensions were measured using a high-precision balance (AUW120D Shimadzu Corp., Japan) and micrometer, respectively [29]. Of these membranes, three were immersed in 75%, 85% and 95% phosphoric acid solutions at 60 °C for 60 min. Five others were immersed in an 85% phosphoric acid solution for 100 min at 40 °C, 10 min at 60 °C, and 5 min at 80, 100 and 120 °C. In order to avoid condensation due to evaporation during heating, the phosphoric acid was kept in a covered container in a water bath at the given temperature. The membranes were removed from the container at intervals, their surfaces were wiped, and their weights and dimensions were measured. In this study, the acid-doping level was defined as the ratio of the "weight of phosphoric acid doped into the membrane" to the "weight of the membrane after doping with phosphoric acid".

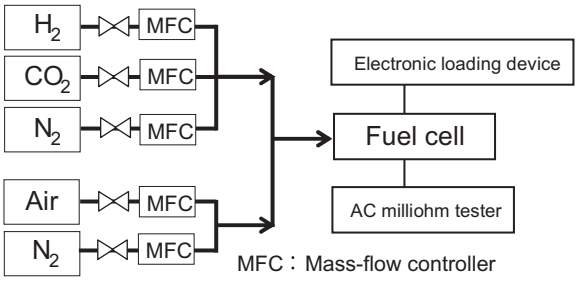

Fig. 1. Schematic diagram of fuel cell station used in this study.

2.2. Preparation of ABPBI electrolyte membranes

ABPBI membranes with dimensions of 5.5 × 5.5 cm^2 and a thickness of 40 μm (FuMA-Tech GmbH, Germany) were prepared. For power generation tests to evaluate the initial cell performance, three electrolyte ABPBI membranes with phosphoric acid doping levels of 68%, 72% and 76% were produced by immersion in an 85% phosphoric acid solution and heating to 40 °C for approximately 6, 8, and 12 min, respectively. For power generation tests to evaluate the long-term durability, two membranes with phosphoric acid doping levels of 78% were produced by immersion in an 85% phosphoric acid solution and heating to 40 °C for approximately 20 min.

2.3. Production of electrodes

A sheet of carbon paper with a thickness of 280 μm (TGP-H-090, Toray Corp., Japan) was used as the gas diffusion layer. A mixed powder of Ketchen Black (EC-600JD, Akzo Nobel Corp., UK) and polytetrafluoroethylene (PTFE; DuPont) in a weight ratio of 65:35 was applied to the carbon paper using a dry coating device [29–31] until a 2 mg cm^{-2} coat was formed. This was then heated at 350 °C in an atmospheric oven, and the surface was leveled by a roller press [29–31] to produce a filled carbon layer.

A catalyst ink was then prepared by mixing polyvinylidene fluoride (PVDF; Kureha Corp., Japan), Pt- and PtCo-supporting Ketchen Black powder (carbon/metal: 50/50, TKK Corp., Japan) [25,26,29] and *N*-methyl pyrrolidone (NMP; Sigma–Aldrich Corp., USA) with agitation for 60 h. To prepare the electrode, the catalyst

Table 1
Membrane and test conditions for Cells A, B, C, D and E used in a previous study [25] and Cell F and G used in this study.

	Cell A	Cell B	Cell C	Cell D	Cell E	Cell F	Cell G
Membrane	PBI					Chemically cross-linked ABPBI	
Cell temp.	150 °C						
Anode	N_2 130 mL min^{-1}	H_2, 130 mL min^{-1}					
Cathode	N_2 130 mL min^{-1}	Air, 310 mL min^{-1}					
Current density	–	0.2 A cm^{-2}					
Generation time (h)	Held for 5 h at 150 °C	2000	12,000	15,000	17,800	1000	17,500
Remarks	Previous study [25]					This study	

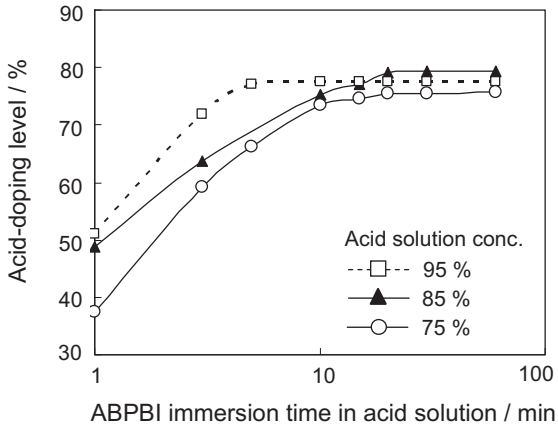

Fig. 2. Influence of phosphoric acid solution concentration and immersion time on acid-doping level of ABPBI at a fixed solution temperature at 60 °C.

ink was applied using a wet-coating method onto carbon paper coated with a mixed powder of carbon and PTFE prepared using a dry-coating method, dried for 1 h at 80 °C in air, and then finally held in a vacuum oven at 160 °C for 25 h to remove the NMP [25,26,29]. The amount of supported Pt was approximately 0.8 mg cm^{-2} for both the anode and cathode electrodes.

2.4. Single cell assembly

To fabricate the MEA, an ABPBI electrolyte membrane doped with phosphoric acid was sandwiched between the two electrodes prepared according to the method described in Section 2.3. This was then sandwiched between a pair of bipolar plates made of carbon, on which a serpentine flow pattern had been machined. The flow pattern was designed by Japan Automobile Research Institute (JARI) and had a reaction area of 5 × 5 cm^2. This assembly was in turn sandwiched between current collector plates and stainless steel end plates, fitted with a rubber heater on the outermost surface, and tightened using eight M6 bolts to produce a single cell [25,26,29]. A total of five single cells were prepared, and were spilt into two groups of three and two, to evaluate the initial cell performance and long-term durability, respectively, during power generation tests. The cells in the latter group were labeled Cells F and G.

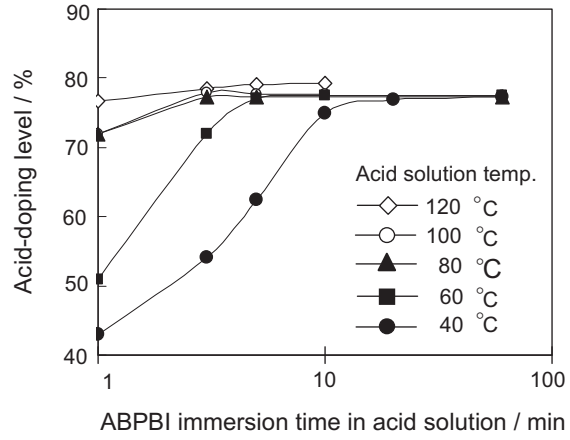

Fig. 3. Influence of phosphoric acid solution temperature and immersion time on acid-doping level of ABPBI for fixed solution concentration of 85%.

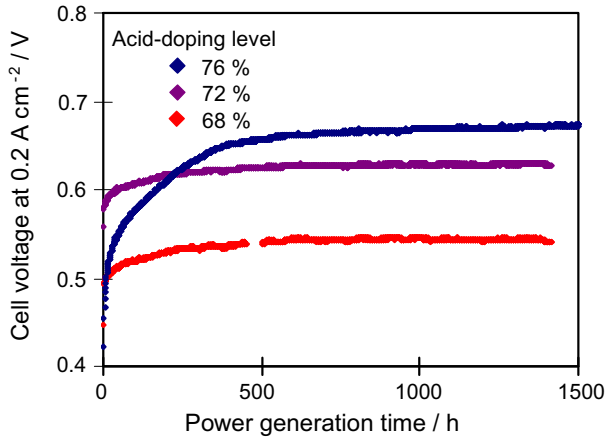

Fig. 4. Change in cell voltage with time for cells with acid-doping levels of 68%, 72% and 76% at 0.2 A cm^{-2} and 150 °C.

2.5. Single cell power generation tests

These five single cells were mounted on a fuel cell test stand (Kofloc Corp., Japan) equipped with mass flow controllers, an electronic loading device (Kikusui Electronics Corp., Japan) for controlling the electric current, an AC milliohm tester (Model 3566, Tsuruga Electric Corp., Japan) operating at a constant frequency of 1 kHz, and a personal computer for equipment monitoring and data output. During all power generation tests, 130 mL min^{-1} (stoich: 3.7) of pure hydrogen and 310 mL min^{-1} (stoich: 3.7) of air were supplied to the anode and cathode sides, respectively, with none of the reaction gases being humidified [25,26,29]. All power generation processes were conducted under atmospheric conditions. Fig. 1 shows a schematic diagram of the fuel cell station used in this study.

To evaluate the dependence of the initial cell performance on the phosphoric acid doping level, power generation tests were conducted on three single cells with phosphoric acid doping levels of 68%, 72% and 76% at a cell temperature of 150 °C and a current density of 0.2 A cm^{-2} for 1400–1500 h until the cell voltage reached its peak value and stabilized.

To evaluate the long-term durability of the cells with ABPBI membranes, power generation tests were conducted on Cell F and G with a phosphoric acid doping level of 78% at a cell temperature of 150 °C and a current density of 0.2 A cm^{-2} for 1000 and 17,500 h,

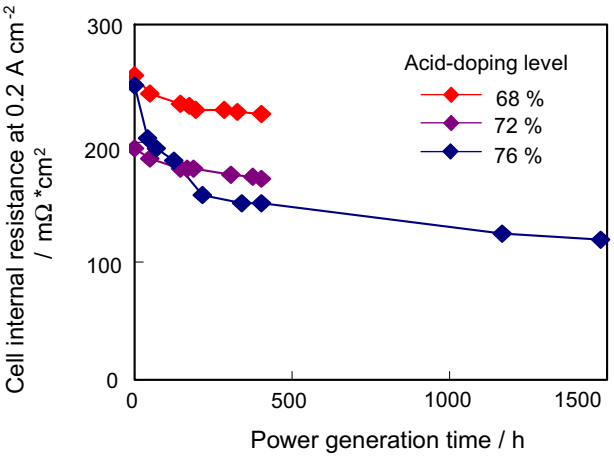

Fig. 5. Change in cell internal resistance with time for cells with acid-doping levels of 68%, 72% and 76% at 0.2 A cm^{-2} and 150 °C.

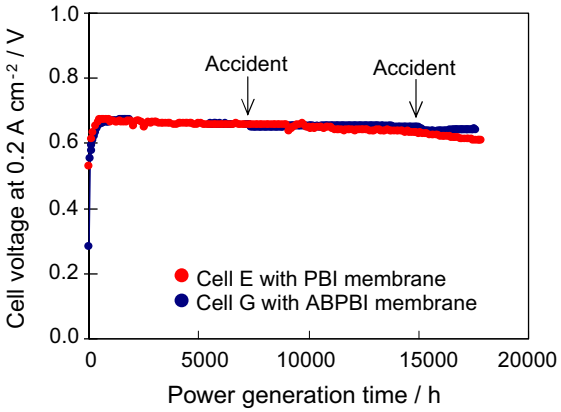

Fig. 6. Change in cell voltage with time during long-term power generation tests on Cell G with ABPBI membrane and Cell E with PBI membrane.

respectively. In this case, the rate of decrease in the cell voltage was calculated based on the difference between the peak cell voltage and that measured during long-term power generation. Table 1 shows the test conditions for Cells F and G together with those for Cells A, B, C, D and E used in a previous study [25].

2.6. Post analysis

As a post analysis of long-term operated MEA, EPMA (EPMA-1610, Shimadzu, Japan) observations were carried out on a cross section of Cell G consisting of the catalyst layer (CL), the gas diffusion layer (GDL) and the microporous layer (MPL) between them.

3. Results

3.1. Acid-doping level

As a preliminary to investigating the influence of the acid-doping level of the ABPBI membranes on the cell voltage, measurements were carried out to verify that the acid-doping level was in fact controllable. Fig. 2 show the change in the acid-doping level in 2 × 2 cm^2 ABPBI membranes with immersion time in 75%, 85% and 95% phosphoric acid solutions at 60 °C. As can be seen, the levels became almost saturated following immersion for 5–10 min in any of the solutions, although the saturation level increased with concentration.

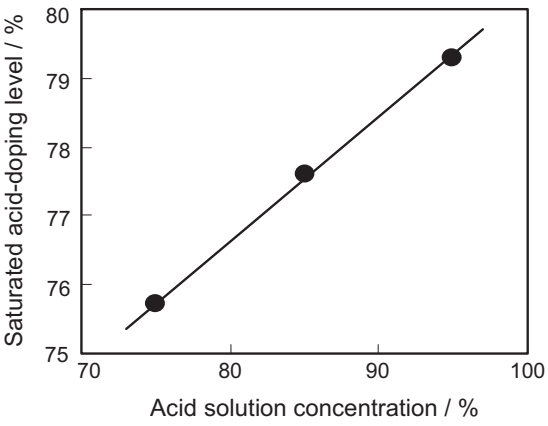

Fig. 7. Relationship between ABPBI saturated acid-doping level and acid solution concentration for immersion at 60 °C.

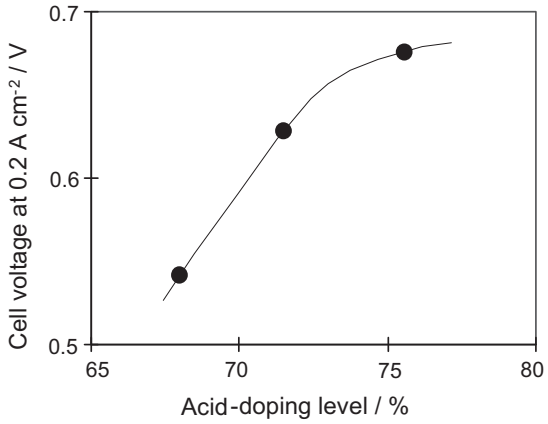

Fig. 8. Relationship between cell voltage at 0.2 A cm^{-2} and acid-doping level for ABPBI membranes.

Fig. 3 shows the change in the acid-doping level with immersion time in 85% phosphoric acid solutions at 40, 60, 80, 100 and 120 °C. It can be clearly seen that, although the acid-doping level saturates at about 78% for all of the samples, the time for saturation to occur increases considerably at lower temperatures. A similar trend was found for PBI in a previous study [29].

3.2. Evaluation of initial cell performance

Figs. 4 and 5 respectively show the change in the cell voltage and internal resistance with time for cells using ABPBI membranes with acid-doping levels of 68%, 72% and 76%, as seen in Fig. 4, the cell voltages increased noticeably during the first few hundreds hours of power generation and then slowly began to saturate. The period of increase is thought to be the time required for evaporation of the solvent in the ABPBI membrane and the CL. As the solvent evaporates, phosphoric acid flows slowly into the resulting pores and the proton conductivity gradually improves.

On the other hand, as shown in Fig. 5, the cell internal resistance initially decreased with time before showing signs of saturation, which is also consistent with solvent evaporation.

3.3. Evaluation of long-term durability

Fig. 6 shows the change in the voltage of Cell G with time during the long-term power generation test. The previously obtained results for Cell E with a PBI membrane are also shown for comparison.

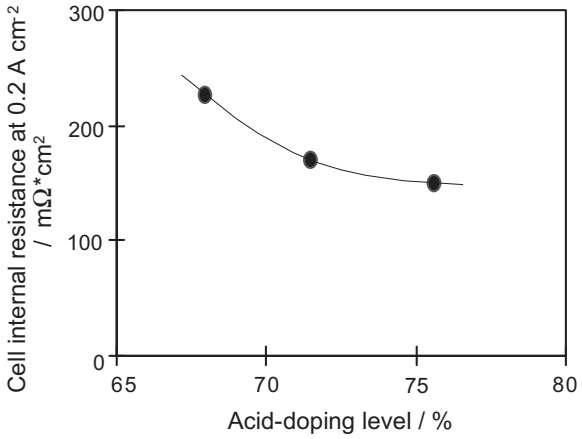

Fig. 9. Relationship between cell internal resistance at 0.2 A cm^{-2} and acid-doping level for ABPBI membranes.

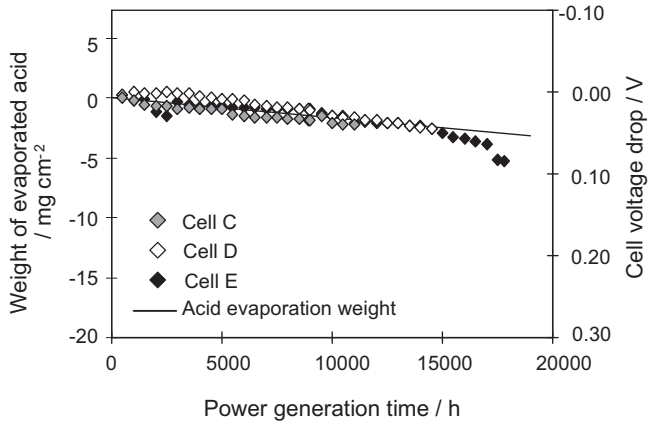

Fig. 10. Long-term power generation test results for Cells C, D and E with PBI membrane operated for 12,000, 15,000 and 17,800 h, respectively [25].

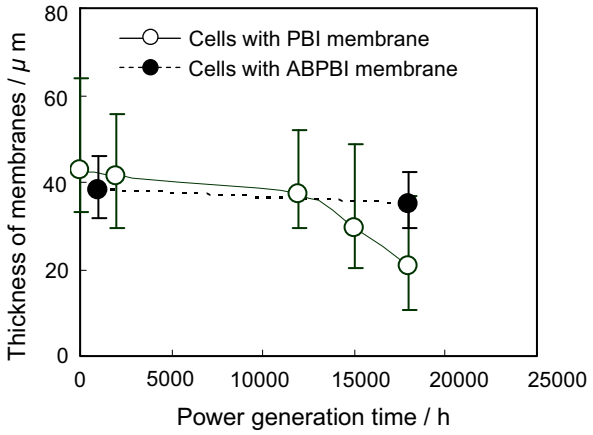

Fig. 12. Changes in membrane thickness with operation time for cells with PBI and ABPBI membranes.

Although Cell G had not yet exhibited a 10% drop in cell voltage from its peak value, the power generation test was terminated at 17,500 h, which is almost the same testing period as for Cell E. In the case of Cell E, the total voltage drop was 68 mV, which represents a decrease of 10% relative to the peak cell voltage of 680 mV. In contrast, for Cell G, a voltage drop of 32 mV occurred, corresponding to a decrease of only 4.4%. In addition, the majority of this decrease was associated with accidental shutdowns of the test station during the testing period, rather than true degradation of the cell.

4. Discussion

4.1. Choice of acid-doping conditions

Fig. 7 shows the relationship between the saturated acid-doping level of ABPBI membranes and the concentration of a 60 °C acid solution. The saturation values are obtained from Fig. 2 for an immersion time of 60 min. For the commonly used immersion

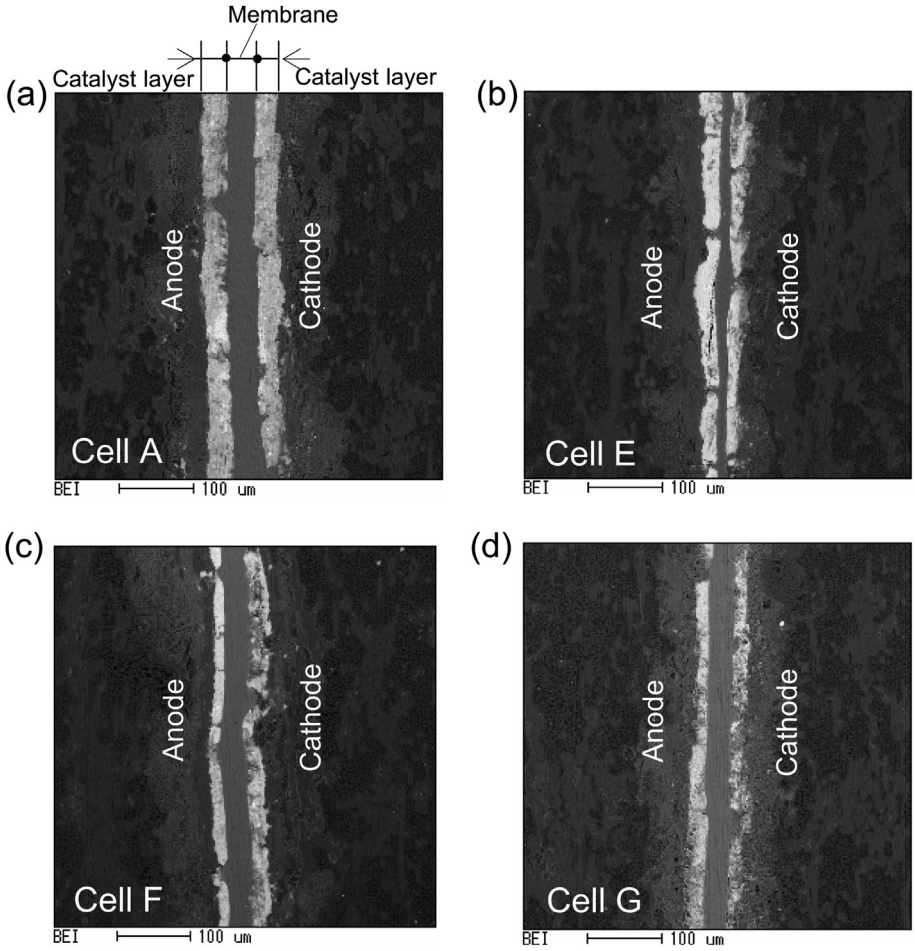

Fig. 11. Cross-sectional SEM images of MEAs from the cells. (a) Cell A with PBI membrane non-operated, (b) Cell E with PBI membrane, operated for 17,800 h, (c) Cell F with ABPBI membrane, operated for 1000 h, and (d) Cell G with ABPBI membrane, operated for 17,500 h.

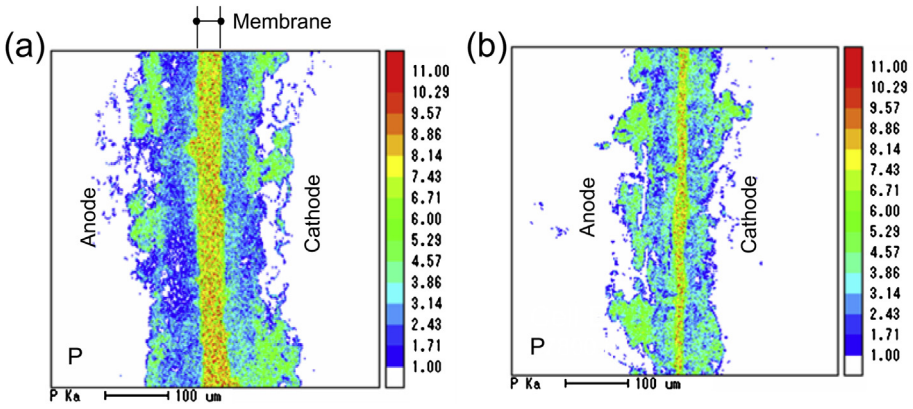

Fig. 13. Cross-sectional EPMA color mapping images for phosphorous in MEAs from cells with PBI membranes. (a) Cell A, non-operated, (b) Cell E, operated for 17,800 h [25].

treatment of 60 min at 60 °C in an 85% phosphoric acid solution, the ABPPI acid-doping level is about 78%.

4.2. Influence of acid-doping level on cell performance

Fig. 8 shows the relationship between the cell voltage following 1200 h of operation at 0.2 A cm^{-2} and the acid-doping level for three cells with ABPBI membranes. The cell voltage data was taken from Figs. 4 and 6. It can be seen that the cell voltage generally increases with acid-doping level, although the increase becomes more gradual at higher doping levels. Judging from the trend in Fig. 8, an acid-doping level of at least 76% is required to achieve a high cell voltage.

Fig. 9 shows the corresponding results for the cell internal resistance following 500 h of operation, where the data for the three cells is taken from Fig. 5. The trend is seen to be opposite to that for the cell voltage.

4.3. Influence of membrane thinning on cell voltage drop

In a previous study [25], it was shown that the drop in voltage for a cell with a PBI membrane during 14,000 h of operation (see Fig. 10) was mainly caused by phosphoric acid depletion due to evaporation. In addition, it was found that the PBI electrolyte membrane was decomposed. The majority of the dissolved PBI had migrated to the catalyst layers, together with a large amount of the phosphoric acid that had been present in the membrane. This decomposition led to a thinning of the PBI membrane, which resulted in cross-leakage of hydrogen and air, and this was thought to cause a faster drop in voltage for operation periods longer than 14,000 h.

In addition, the results of the same study indicated that this accelerated voltage drop was not strongly influenced by an increase in the electrocatalyst particle size [21]. In fact, as shown in Fig. 6, although the voltage of Cell E with the PBI membrane decreased by 10% during 17,800 h of operation, that of Cell G with the ABPBI membrane decreased by only 4.4% during 17,500 h of operation, and this was mainly due to two accidental shutdowns of the test station that caused phosphoric acid to leak from the cell as its temperature decreased to room temperature. Since the difference between Cell E and Cell G was the type of membrane used, these results also support the idea that the accelerated voltage drop was caused by degradation of the PBI membrane rather than an increase in the electrocatalyst particle size.

To confirm this, an EPMA post-analysis was carried out on cross sections of MEAs removed from Cell F and G, following operation for 1000 and 17,500 h, respectively. The results were then compared with those previously obtained for Cell A and Cell E with PBI membranes, following operation for 0 and 17,800 h, respectively [25]. Fig. 11(a)–(d) shows cross-sectional SEM images of MEAs from Cells A, E, F and G, respectively, following the power generation tests. It can be seen that for the cells with the PBI membranes, a large decrease in the membrane thickness occurred between 0 and 17,800 h of operation. However, this is not the case for the cells with the ABPBI membranes, for which almost no change in membrane thickness is observed between 1000 and 17,500 h of operation. These results verify that decomposition and thinning can be suppressed by chemical cross-linking.

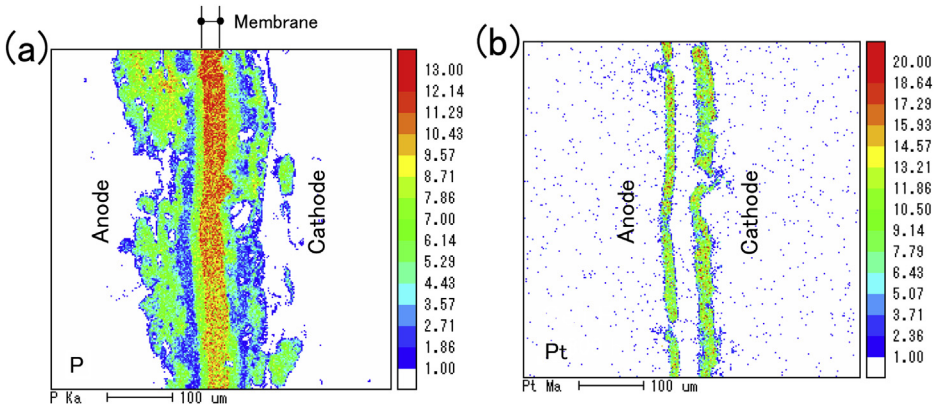

Fig. 14. Cross-sectional EPMA of MEA from Cell F with ABPBI membrane, operated for 1000 h. (a) Color mapping for phosphorous, (b) color mapping for platinum.

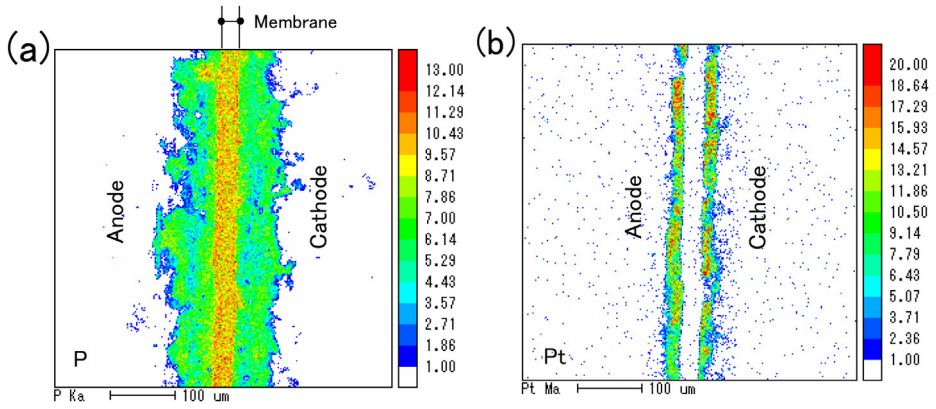

Fig. 15. Cross-sectional EPMA of MEA from Cell G with ABPBI membrane, operated for 17,500 h. (a) Color mapping for phosphorous, (b) color mapping for platinum.

Fig. 12 shows the change in membrane thickness as a function of final operation time for Cells A to E and Cells F to G. Each point represents an average of fifty measurements of the membrane thickness from the SEM images, with the spread in values being represented by the error bars. It can be seen that for the PBI membranes, the thinning process begins to accelerate at about 14,000 h. On the other hand, for the ABPBI membranes, almost no thinning is observed over the entire test period.

Fig. 13(a) and (b) shows cross-sectional EPMA elemental mapping images for phosphorous in MEAs from Cells A and E, respectively. Again, clear membrane thinning is apparent after 17,800 h of operation, and a decrease in phosphoric acid concentration has occurred not only in the catalyst layers but also in both gas diffusion layers.

Fig. 14(a) and (b) shows cross-sectional EPMA color mapping images for phosphorous and platinum, respectively, in the MEA from Cell F following 1000 h of operation. Fig. 15(a) and (b) shows the corresponding images for Cell G following 17,500 h of operation. Comparing Fig. 14(a) and Fig. 15(a), it is clear that the thickness of the ABPBI membrane has not changed and the phosphoric acid concentration has remained high in the catalyst and gas diffusion layers. Furthermore, a comparison of Fig. 14(b) and Fig. 15(b) show that the platinum content in the electrocatalysts has remained relatively constant during operation.

5. Conclusion

Power generation tests were carried out on HT-PEMFCs with ABPBI membranes doped with phosphoric acid to levels of 62%, 72% and 76% in order to evaluate the influence of the acid-doping level on cell performance. Tests were also carried out on two cells with an acid-doping level of 78% at a current density of 0.2 A cm^{-2} for 1000 and 17,500 h in order to verify that the stability of the electrolyte membrane has the main influence on the durability of HT-PEMFCs up to around 20,000 h. The latter cells were post-analyzed using SEM and EPMA. The results were compared with those for cells with PBI membranes, allowing the mechanism of cell performance reduction in HT-PEMFCs to be clarified.

The long-term test results showed although a voltage decrease of 10% occurred for the cell with the PBI membrane, the decrease was only 4.4% for the cell with the ABPBI membrane, and this was mainly due to accidental shutdowns of the test station during the testing period.

The results of the post-analysis indicated that, following cell operation for 17,500 h, the ABPBI membrane maintained its original thickness, and that the phosphoric acid remained high both in catalyst layers the gas diffusion layers. In addition, the platinum content in the electrocatalyst remained constant.

The reason why ABPBI's cell showed better performance than PBI's cell will be discussed in the next stage.

References

[1] T. Shimizu, in: 7th Int'l Hydrogen & Fuel Cell Expo, FC-4 (2011), p. 18.
[2] P. Krishnan, J.S. Park, C.S. Kim, J. Power Sources 159 (2006) 817.
[3] H. Xu, Y. Song, H.R. Kunz, J.M. Fenton, J. Power Sources 159 (2006) 979.
[4] C.P. Wang, H.S. Chu, Y.Y. Yan, K.L. Hsueh, J. Power Sources 170 (2007) 235.
[5] J. Karstedt, J. Ogrzewalla, C. Severin, S. Pischinger, J. Power Sources 196 (2011) 9998.
[6] D. Plackett, A. Siu, Q. Li, C. Pan, C. Pan, J.O. Jensen, S.F. Nielson, A.A. Permyakova, N.J. Bjerrum, J. Membr. Sci. 383 (2011) 78.
[7] J. Lobato, P. Canizares, M.A. Rodrigo, D. Ubeda, F.J. Pinar, J. Membr. Sci. 369 (2011) 105.
[8] J. Hu, J. Luo, P. Wagner, O. Conrad, C. Agert, Electrochem. Commun. 11 (2009) 2324.
[9] R. Bouchet, E. Siebert, Solid State Ionics 118 (1999) 287.
[10] B. Xing, O. Savadogo, Electrochem. Commun. 2 (2000) 697.
[11] P. Donoso, W. Gorecki, C. Berthier, F. Defendini, C. Poinsignon, M. Armand, Solid State Ionics 28–30 (1988) 969.
[12] M.S. Boroglu, S.U. Celik, A. Bozkurt, I. Boz, J. Membr. Sci. 375 (2011) 157.
[13] S. Zeng, L. Ye, S. Yan, G. Wu, Y. Xiong, W. Xu, J. Membr. Sci. 367 (2011) 78.
[14] D. Rogriguez, C. Jegat, O. Trinquet, J. Grondin, J.C. Lassegues, Solid State Ionics 61 (1993) 195.
[15] M.F. Daniel, B. Desbat, F. Cruege, O. Trinquet, J.C. Lassegues, Solid State Ionics 28–30 (1988) 637.
[16] J.A. Asensio, S. Borros, P.G. Romero, J. Electrochem. Soc. 151 (2) (2004) A304.
[17] J.R.P. Jayakody, S.H. Chung, L. Durantio, H. Zhang, L. Xiao, B.C. Benicewicz, S.G. Greenbaum, J. Electrochem. Soc. 154 (2007) B242.
[18] Q. Li, J.O. Jensen, R.F. Savinell, N.J. Bjerrum, Prog. Polym. Sci. 34 (2) (2009) 449.
[19] J. Parrondo, F. Mijangos, B. Rambabu, J. Power Sources 195 (2010) 3977.
[20] J. Lobato, P. Canizares, M.A. Rodrigo, D. Ubeda, F.J. Pinar, J. Power Sources 196 (2011) 8265.
[21] Y. Zhai, H. Zhang, D. Xing, Z.G. Shao, J. Power Sources 164 (2007) 126.
[22] J. Zhang, Y. Tang, C. Song, J. Zhang, J. Power Sources 172 (2007) 163.
[23] A. Sounai, K. Sakai, in: Proceedings of the 13th Fuel Cell FCDIC Symposium, 2006, p. 125.
[24] J. Baurmeister, T. Kohno, in: Proceedings of the 13th Fuel Cell FCDIC Symposium, 2006, p. 122.
[25] Y. Oono, A. Sounai, M. Hori, J. Power Sources 210 (2012) 366.
[26] Y. Oono, T. Fukuda, A. Sounai, M. Hori, J. Power Sources 195 (2010) 1007.
[27] L.A. Diaz, G.C. Abuin, H.R. Corti, J. Power Sources 188 (2009) 45.
[28] J.A. Asensio, P. G-Romero, Fuel Cells 5 (3) (2005) 336.
[29] Y. Oono, A. Sounai, M. Hori, J. Power Sources 189 (2009) 943.
[30] J. Yu, Y. Yoshikawa, T. Matsuura, M.N. Islam, M. Hori, Electrochem. Solid State Lett. 8 (3) (2005) A152.
[31] J. Yu, T. Matsuura, Y. Yoshikawa, M.N. Islam, M. Hori, Electrochem. Solid State Lett. 8 (3) (2005) A156.